Radiological Imaging of Viral Pneumonia Cases Identified Before the COVİD-19 Pandemic Period and COVİD-19 Pneumonia Cases Comparison of Characteristics

Authors

1. Rana Günöz Cömert Istanbul University, Istanbul Faculty of Medicine, Radiology Department, M.D., Radiology Specialist

   rgcomert@gmail.com

   https://orcid.org/0000-0003-3084-8232

2. Eda Cingöz

   Istanbul University, Istanbul Faculty of Medicine, Radiology Department, M.D.

   edacanipek@gmail.com

   https://orcid.org/0000-0003-0814-4597

3. Sevim Meşe

   Istanbul University, Istanbul Faculty of Medicine, Department of Medical Microbiology,

   Associate Professor M.D.

   drsevimmese@gmail.com

   https://orcid.org/0000-0001-5944-0180

4. Görkem Durak

   Istanbul University, Istanbul Faculty of Medicine, Radiology Department, M.D.

   grkmitf@hotmail.com

   https://orcid.org/0000-0002-1608-1955

5. Atadan Tunacı

   Istanbul University, Istanbul Faculty of Medicine, Radiology Department, Prof. M.D.

   atatuna@gmail.com

   https://orcid.org/0000-0002-8796-8641

6. Ali Ağaçfidan

   Istanbul University, Istanbul Faculty of Medicine, Department of Medical Microbiology, Prof. Dr.

   aagacfidan@hotmail.com

   https://orcid.org/0000-0002-5470-296X

7. Mustafa Önel

   Istanbul University, Istanbul Faculty of Medicine, Department of Medical Microbiology, Ph.D.

   aslanmus70@hotmail.com

   https://orcid.org/ 0000-0002-3987-6611

8. Şükrü Mehmet Ertürk

   Istanbul University, Istanbul Faculty of Medicine, Radiology Department, Prof. M.D.

   smerturk@gmail.com

   https://orcid.org/0000-0001-6008-5454

Radiological Imaging of Viral Pneumonia Cases Identified Before the COVİD-19 Pandemic Period and COVİD-19 Pneumonia Cases Comparison of Characteristics

Abstract

Background: Thoracic CT imaging is widely used as a diagnostic method in the diagnosis of COVID-19 pneumonia. Radiological differential diagnosis and isolation of other viral agents causing pneumonia in patients gained importance, especially during the pandemic period.

Aims: We aimed to investigate whether there is a difference between the CT imaging findings characteristically defined in COVID-19 pneumonia and the findings detected in pneumonia due to other viral agents, and which finding may be more effective in the diagnosis.

Study Design: The study included 249 adult patients with pneumonia found in thorax CT examination and positive COVID-19 RT-PCR test and 94 patients diagnosed with non-COVID pneumonia (viral PCR positive, no bacterial/fungal agents were detected in other cultures) from the last 5 years before the pandemic. It was retrospectively analyzed using the PACS System. CT findings were evaluated by two radiologists with 5 and 20 years of experience who did not know to which group the patient belonged, and it was decided by consensus.

Methods: Demographic data (age, gender, known chronic disease) and CT imaging findings (percentage of involvement, number of lesions, distribution preference, dominant pattern, ground-glass opacity distribution pattern, nodule, tree in bud sign, interstitial changes, crazy paving sign, reversed halo sign, vacuolar sign, halo sign, vascular enlargement, linear opacities, traction bronchiectasis, peribronchial wall thickness, air trapping, pleural retraction, pleural effusion, pericardial effusion, cavitation, mediastinal/hilar lymphadenopathy, dominant lesion size, consolidation, subpleural curvilinear opacities, air bronchogram, pleural thickening) of the patients were evaluated. CT findings were also evaluated with the RSNA consensus guideline and the CORADS scoring system. Data were divided into two main groups as non-COVID-19 and COVID-19 pneumonia and compared statistically with chi-square tests and multiple regression analysis of independent variables.

Results: Two main groups; RSNA and CORADS classification, percentage of involvement, number of lesions, distribution preference, dominant pattern, nodule, tree in bud, interstitial changes, crazy paving, reverse halo vascular enlargement, peribronchial wall thickness, air trapping, pleural retraction, pleural/pericardial effusion, cavitation and mediastinal/hilar lymphadenopathy were compared, significant differences were found between the groups ($p < 0.01$). Multiple linear regression analysis of independent variables found a significant effect of reverse halo sign ($\beta = 0.097$, $p < 0.05$) and pleural effusion ($\beta = 10.631$, $p < 0.05$) on COVID-19 pneumonia.

Conclusion: Presence of reverse halo and absence of pleural effusion was found to be efficient in the diagnosis of COVID-19 pneumonia.

Keywords: COVID-19, Viral Pneumonia, Computed Tomography, Thorax Radiology

Introduction

Viruses are the most common cause of respiratory tract infections. It has been reported that viruses such as influenza, HPIV, Adenovirus, RSV, HMPV can cause lower respiratory tract infections in individuals with both normal immune systems and immunodeficiency; It is known that viruses such as rhinovirus, endemic coronaviruses, CMV, Herpes Simplex Virus (HSV), Varicella Zoster Virus (VZV), HBoV can cause lower respiratory tract infection only in those with immunodeficiency.[1]

Coronavirus disease (COVID) was first reported by the World Health Organization (WHO) on December 31, 2019, with pneumonia cases of unknown origin being reported in Wuhan, China, and then reached the pandemic stage in March 2020.[2]

SARS-CoV-2, the causative agent of COVID-19 disease, is an enveloped virus whose genetic material consists of single-stranded RNA. The RT-PCR test, in which viral nucleic acid is detected, is accepted as the gold standard for the detection of SARS-CoV-2 virus.[3]

It is reported that COVID-19 infection can be examined in 3 stages, including the first asymptomatic period, secondly the upper and lower respiratory tract response, and then widespread lung involvement that can progress to ARDS.[4] In the COVID-19 disease, approximately 80% of the patients are asymptomatic or limited to mild to moderate symptoms in the first two stages; It is reported that in the remaining 15-20% of the patients, pulmonary ground glass opacity-consolidation is detected as a radiological finding due to the inflammatory response in the lung.[4]

If there is no risk factor for the progression of the disease in patients with mild clinical symptoms suspicious for COVID-19, there is no imaging indication, and imaging should be performed in cases with worsening respiratory system symptoms; It has been reported that imaging can be performed to provide medical triage in cases with high suspicion for COVID-19 with moderate-to-severe symptoms if clinical conditions require it.[5]

A normal chest X-ray does not exclude COVID-19 pneumonia, especially in cases with mild pneumonia or in the early stage of the disease.[5,6] It has been reported that CT cannot be used

as a screening test, since the positive predictive value of thoracic CT in the diagnosis of COVID-19 is 92% high while the negative predictive value is 42% [7] and the absence of CT findings in the early phase of the disease should not exclude the possibility of COVID-19 disease.[2,8] Clinical It has been reported that the combination of repetitive RT-PCR test and thoracic CT examination is beneficial in cases with suspected COVID-19.[9]

Imaging findings of viral pneumonia may overlap with non-viral infections and inflammatory conditions. Some diagnostic patterns of viral pneumonia help to make differential diagnoses in the early stages of infection, to reduce unnecessary antibiotic use, and to prevent contagion.[1] In thorax CT in viral pneumonia; reticular opacities due to interstitial inflammation, ground-glass opacity(GGO) due to alveolar edema, patchy consolidation, localized atelectasis, peribronchovascular thickening, centrilobular nodular opacities, tree in bud pattern, interlobular septal thickening, etc. findings develop, but it is reported that diagnosis cannot be made based on imaging findings alone.[10,11] However, detection of centrilobular nodular opacities, pleural effusion, and lymphadenopathy more frequently in non-COVID-19 viral pneumonia has been reported to help differential diagnosis.[11]

Computed tomography of the thorax is used as a common diagnosis method in the diagnosis of Coronavirus Disease 2019 (COVID-19) which causes pandemics. As in the pre-pandemic period, during the COVID-19 pandemic period, the radiological differential diagnosis of other viral agents that cause pneumonia in patients with normal immunity or in immunosuppressed patients with seasonal epidemics has gained importance in early diagnosis and isolation. Therefore, it was aimed to investigate the difference between CT imaging findings defined as characteristic in COVID-19 pneumonia and CT findings detected in pneumonia due to other viral agents previously encountered.

Materials and Methods

Researched Patient Population:

As the COVID group, 249 COVID-19 patients aged 18 years and older, who applied to our hospital, were found to have positive Reverse Transcriptase Polymerase Chain Reaction (RT-PCR) in the nasopharyngeal swab samples taken at the application, and pneumonia was detected in the thorax CT examination at admission has been included.

For the non-COVID group, viral respiratory panel or bronchoalveolar lavage/blood viral PCR results within an average of 5.67±7.95 days, from the last 5 years before the pandemic, 18 years of age and older, with thorax CT findings compatible with viral pneumonia 94 patients who were positive but no bacterial or fungal agents were detected in other sputum and blood cultures (Viral panel results; Influenza AB n=26, Adenovirus n=5, CMV n=28, RSV n=8, Parainfluenza n=10, HMPV n=3 , Endemic Coronaviruses (HCoV-NL63, HCoV-HKU, HCoV-229E, HCoV-OC43) n=16, Rhinovirus n=7, Bokavirus (HBoV) n=1) were included in the study.

Laboratory PCR Test Method:

FTD Respiratory pathogens 21 (fast-tract DIAGNOSTICS, Luxembourg) kit, which is based on the reverse transcriptase Multiplex PCR method, was used for the Viral Respiratory Panel. Artus CMV QS-RGQ kit QIAsymphony RGQ system (QIAGEN) as a CMV DNA quantitative test between January 2015 and September 2018 (measuring range of the kit: 79.4 copies / mL-100,000,000 copies / mL, 1 copy / mL = 1.64 IU / mL), COBAS Ampliprep / taqman CMV test and COBAS Ampliprep / Taqman system were used between September

2018 and December 2019 (measuring range of the kit: 150 copies / mL-10000000 copies / mL, 1 copy / mL = 0.91 IU / mL).

Viral RNA extraction from respiratory samples of patients with COVID-19 symptoms was performed manually with Bio-Speedy® Viral Nucleic Acid Isolation Kit (Bioeksen R&D Technologies Company; Turkey). RT-qPCR procedure was performed on Rotor-Gene Q 5 Plex Real Time PCR (Qiagen, Germany) using Bio-Speedy® COVID-19 RT-qPCR Detection Kit (Bioeksen Ar-Ge Technologies Company; Turkey). In the working principle of this kit, human ribonuclease P (RNA ace p) gene is targeted as an internal control. The positivity of RNAse P allows evaluation of the RT-qPCR process by confirming the extraction process, and the SARS-CoV-2 PCR result is interpreted as positive with the detection of the amplification curve of the RdRp gene region.

Thorax CT Examination Protocol, Evaluation and Statistical Analysis

Thorax CT examination protocol; tube voltage 120kV with 64 detectors, Aquillion, Toshiba and 16 detectors Brilliance, Philips; tube current modulation 50-150 mA; range 0.85-1.4; image slice thickness is 1 mm-5 mm, CT images obtained in the supine position in full inspiratory in all patients are -600 to +1600 HU for lung parenchyma, +50 to +350 HU for mediastinum using window width; it was retrospectively analyzed using the PACS System. CT findings were evaluated by two radiologists with 5 and 20 years of experience who did not know to which group the patient belonged, and it was decided by consensus.

Age, gender, known chronic disease of the patients; CT findings include the percentage of involvement, number of lesions, distribution preference, dominant pattern, ground-glass opacity distribution pattern, nodule, tree in bud sign, interstitial changes, crazy paving sign, reversed halo sign, vacuolar sign, halo sign, vascular enlargement (vascular structures with

increased calibration relative to the proximal, which is thought to be due to mediators that cause hyperemia, in the area of inflammation or in the periphery of the lesion [12]), linear opacities, traction bronchiectasis, peribronchial wall thickness, air trapping, pleural retraction, pleural effusion, pericardial effusion, cavitation, mediastinal/hilar lymphadenopathy, dominant lesion size, consolidation, subpleural curvilinear opacities, air bronchogram, pleural thickening were examined. CT findings were also evaluated with the RSNA consensus guideline and the CORADS scoring system, data obtained were divided into two main groups as non-COVID-19 pneumonia and COVID-19 pneumonia; statistically compared with chi-square tests and multiple regression analysis of independent variables.

Results

In the study, the age ranged between 18 and 91, with a mean of 51.99±16.99, with a median value of 53. The age of the non-COVID-19 patient group ranged from 18 to 84, with a mean of 49.29±19.43. The age of the COVID-19 patient group ranged from 18 to 91, with a mean of 53.01±15.91. In the study, 59.5% (n=204) of the patients were male, while 40.5% (n=139) were female. While 58.5% (n=55) of the non-COVID-19 pneumonia patient group were male, 41.5% (n=39) were female. Of the COVID-19 pneumonia patient group, 59.8% (n=149) were male, while 40.2% (n=100) were female. (Table 1)

While 33% (n=113) of the COVID-19 patient group had no chronic disease, the entire non-COVID-19 patient group (n=94) had chronic diseases. Concomitant chronic diseases of COVID-19 patients including cardiovascular disease (%4,1 n=14) vs (%3,7 n=4); hypertension (%22,5 n=77) vs (%1,9 n=2); diabetes mellitus (%14,6 n=50) vs (%5,6 n=6); chronic lung disease (%1,8 n=6) vs (%2,8 n=3); chronic liver disease (%0, n=0) vs (%1,9

n=2); chronic kidney disease (%2,3 n=8) vs (%19,4 n=21); extrapulmonary malignancy (%3,2 n=11) vs (%21,3 n=23); conditions related to immunodeficiency (%3,5 n=12) vs (%28,7 n=31); others (%14,9 n=51) vs (%14,8 n=16) compared to non-COVID-19 patients. (Table 1)

In COVID-19 patients finding including RSNA typical group (%85,9 n=214) vs (%40,4 n=38); RSNA indetermine group (%11,7 n=29) vs (%34 n=32); CORADS 5 score (%77,9 n=194) vs (%26,6 n=25), CORADS 4 score (%12,4 n=31) vs (%12,8 n=12), CORADS 3 score (%6,8 n=17) vs (%31,9 n=30), CORADS 2 score (%2,8 n=7) vs (%28,7 n=27) compared to non-COVID-19 patients ($p<0,01$). (Table 2)

In COVID-19 patients finding including percentage of involvement %75< (%4,4 n=11) vs (%17, n = 16), %50-%75 (%13,7 n=34) vs (%18,1 n=17), %25-%50 (%39 n=97) vs (%30,9 n=29), %0-%25 (%43 n=107) vs (%34 n=32); single lesion (%6,8 n=17) vs (%1,1 n=1); peripheral+ central distribution (%40,7 n=101) vs (%11,7 n=11); where the dominant pattern is ground glass (%78,7 n=196) vs (%56,4 n=53), consolidation (%18,5 n=46) vs (%13,8 n=13), linear-reticular opacities (%1,2 n=3) vs (%2,1 n=2), nodules (%1,6 n=4) vs (%27,7 n=26); distribution pattern of GGO absence (%1,2 n=3) vs (%10,6 n=10), peripheral-bilateral (%56,2 n=140) vs (%20,2 n=19), round-multifocal (%27,3 n=68) vs (%21,3 n=20), halo sign (%0 n=0) vs (%1,1 n=1), diffuse (%1,6 n=4) vs (%27,7 n=26), perihilar-not round (%1,2 n=3) vs (%5,3 n=5), single sided- not round (%12,4 n=31) vs (%13,8 n=13); presence of nodule (%4,8 n=12) vs (%60,6 n=56); tree in bud pattern (%3,2 n=8) vs (%52,1 n=49); interstitial changes absent (%24,1 n=60) vs (%25,5 n=24), septal thickening (%6,8 n=17) vs (%35,1 n=33), fine reticular opacity (%28,9 n=72) vs (%7,4 n=7), both septal thickening and fine reticular opacity (%40,2 n=100) vs (%31,9 n=30); crazy paving pattern (%30,5 n=76) vs

(%13,8 n=13); reversed halo (%43,8 n=109) vs (%6,4 n=6); microvascular enlargement (%83,1 n=207) vs (%63,8 n=60); linear opacities (%63,1 n=157) vs (%75,5 n=71); traction bronchiectasis (%62,2 n=155) vs (%47,9 n=45); peribronchial wall thickening (%32,9 n=82) vs (%58,5 n=55); air trapping (%11,6 n=29) vs (%33 n=31); pleural retraction (%39,8 n=99) vs (%57,4 n=54); pleural effusion (%3,2 n=8) vs (%33 n=31); pericardial effusion (%3,6 n=9) vs (%29,8 n=28); cavitation (%0 n=0) vs (%3,2 n=3); mediastinal lymph node nonspecific (%92 n=229) vs (%69,1 n=65), pathological (%8 n= 20) vs (%29,8 n=28), another reason (%0 n=0) vs (%1 n=1) compared to non-COVID-19 patients (p<0,01). (Table 2)

In COVID-19 patients finding including dominant lesion size 0-3 cm (%34,1 n=85) vs (%45,7 n=43), 3-5 cm (%18,5 n=46) vs (%10,6 n=10), 5-7 cm (%12 n=30) vs (%8,5 n=8), >7 cm (%35,3 n=88) vs (%35,1 n=33); consolidation (%55 n=137) vs (%55,3 n=52); vacuolar sign (%8,8 n=22) vs (%11,7 n=11); halo sign (%24,2 n=60) vs (%20,2 n=19); subpleural curvilinear opacity (%30,1 n=75) vs (%24,5 n=23); air bronchogram (%19,8 n=49) vs (%24,5 n=23); pleural thickening (%21,7 n=54) vs (%20,2 n=19) compared to non-COVID-19 patients (p>0,05). (Table 2)

In the multiple linear regression analysis performed to determine the effect of independent variables on COVID-19 pneumonia; when the regression coefficients were examined, it was found that those with reversed halo sign ($\beta = 0.097$, $p < 0.05$) and those with pleural effusion ($\beta = 10.631$, $p < 0.05$) had a significant effect on COVID-19 pneumonia; it was found that COVID-19 pneumonia was more common in patients with reversed halo sign compared to those without pleural effusion. (Table 3)

Discussion and Conclusion

The gold standard method in the screening and diagnosis of COVID-19 is the RT-PCR test. Since the thorax CT examination is the most commonly used method in clinical practice after the RT-PCR test in the diagnosis of COVID-19, it was aimed to investigate whether the characteristic imaging findings diagnosed for COVID-19 pneumonia and whether the classification systems established for the standardization of these findings differ from the CT findings detected in pneumonia due to other viral agents.

Pleural effusion is a more common finding in non-COVID-19 viral pneumonia than in COVID-19 pneumonia[11] (Figure 1). Although this information supports our results, in our study, all of the patients with non-COVID-19 viral pneumonia had concomitant chronic diseases, while 33% (n = 113) of the patient group with COVID-19 pneumonia had no chronic disease. The higher prevalence of diseases such as cardiovascular disease, chronic renal failure, extrapulmonary malignancy, and immunodeficiency-related conditions (73.1% vs 13.1%) in the non-COVID-19 viral pneumonia patient group also contributed to the significance of pleural effusion as a result of regression analysis may have been found.

While COVID-19 pneumonia often involves peripheral (Figure 2.); central or random multilobar distribution with peribronchovascular pure consolidation is observed in influenza pneumonia (Figure 3., 4., 5.). In addition, it is reported that the presence of round opacities, interlobular septal thickenings/ crazy paving, sharper lesion margin, and the absence of nodule/tree in bud appearance are helpful features for COVID-19 pneumonia to distinguish it from influenza. [13],[14],[15]

In the literature, there is information that the pulmonary target sign, which is defined as a variant of the reversed halo sign by making a difference with the hyperdense dot sign in the center, is diagnostic in COVID-19 viral pneumonia.[16,17] In our study, we did not evaluate the presence of central hyperdense dot as a separate parameter, but we think that we contributed to the literature by concluding that the presence of the reversed halo sign is valuable in differentiating other viral pneumonia from COVID-19. (Figure 6.)

In the literature[18], it has been reported that CT findings of Adenovirus pneumonia and COVID-19 pneumonia (segmental and subpleural consolidations, air bronchogram, interlobular septal thickening, accompanying mildly limited GGO and pleural effusion) overlap. (Figure 7)

Compared with a study [19] conducted with COVID-19 patients whose diagnosis was confirmed by RT-PCR and who had pneumonia on thorax CT and non-COVID-19 patients whose respiratory panel PCR was positive and pneumonia on CT, our study differed from COVID-19. We compared two groups without COVID-19 for the RSNA consensus guideline and the CORADS system.

Classification recommendations such as RSNA consensus guideline [2], CORADS [20],[21] have been brought to the agenda in the pandemic process with the aim of defining the imaging findings in a standard way in patients who are investigated for COVID-19 pneumonia and creating a standardized reporting language in order to provide clarity in communication with other branches for patient management by reducing uncertainty in reports. Studies evaluating the diagnostic performance of CORADS report a consistent evaluation system with high positive predictions.[8],[22],[23],[24],[25] In the literature, there is no study comparing the findings of

COVID-19 pneumonia in terms of RSNA consensus guideline and CORADS with patients diagnosed with non-COVID-19 viral pneumonia as in our study. According to the RSNA consensus guidelines; the scores of atypical group and CORADS 2, indetermined group and CORADS 3 correspond to each other and were found to be significant in favor of non-COVID-19 viral pneumonia. The RSNA typical group and the CORADS 5 score also correspond to each other and were found to be similarly significant in favor of COVID-19 pneumonia. We think that the lack of diagnostic difference between the groups in the CORADS 4 score may be due to the fact that frequent findings in other viral pneumonia such as small but peripherally localized unilateral GGO and multifocal consolidation without other typical findings are included in this category. Although it has been reported in studies reporting that dividing the RSNA indeterminate category into 3 and 4 in the CORADS system limits the intra-observer variability[8], since these assessment systems were developed during the pandemic process, when the prevalence of COVID-19 decreases after the pandemic is over, it is an issue that needs to be studied how much it can be applied to incidental thoracic CT findings independent of the clinic and In the future, these studies may contribute to improving the diagnostic efficiency of CORADS.

The low number of parameters affecting the result in regression analysis may be due to the low number of patients. The limited number of patients is associated with inclusion of patients with positive PCR test and proven diagnosis in the study, exclusion of cases with concomitant bacterial and fungal infections for the patient group with non-COVID-19 viral pneumonia, and the fact that patients presenting with respiratory tract infection symptoms before the COVID-19 pandemic are not performed as frequently as today, chest CT scans. The hospital information system data of the patient group diagnosed with non-COVID-19

viral pneumonia from the last 5 years before the pandemic were retrospectively scanned, and the thorax CT imaging closest to the date of PCR test was evaluated, but the CT-laboratory time interval in this group is longer than the COVID-19 pandemic period. Since the non-COVID-19 viral pneumonia group includes 5 years retrospectively, access to information about the time from the onset of symptoms to imaging is limited. The presence of co-infection in patients diagnosed with COVID-19 pneumonia is not known since most of these patients did not have additional microbial culture examinations during the pandemic period, but we expect that the presence of hospital-acquired coinfection will be lower since we have evaluated the first thorax CT examinations of these patients diagnosed with COVID-19 pneumonia.

In conclusıon**;** ın the diagnosis of viral pneumonia, radiological imaging, which is evaluated together with laboratory examinations, especially clinical and gold-standard RT-PCR test, has an important role in diagnosis and patient management. RSNA classification and CORADS scoring system can be used to distinguish COVID-19 pneumonia from non-COVID-19 pneumonia. The presence of reversed halo sign and absence of pleural effusion was found to be efficient in the diagnosis of COVID-19 pneumonia.

Conflicts of Interest: There is no conflict of interest between the authors.

Funding Statement: No supporting funds were used for our study.

References

1. Koo HJ, Lim S, Choe J, et al. Radiographic and CT features of viral pneumonia. *Radiographics* 2018; 38: 719–739.
2. Gorbalenya AE, Baker SC, Baric RS, et al. Covid-19&Ct.
3. Carter LJ, Garner L V., Smoot JW, et al. Assay Techniques and Test Development for COVID-19 Diagnosis. *ACS Cent Sci* 2020; 6: 591–605.
4. Mason RJ. Pathogenesis of COVID-19 from a cell biology perspective. *Eur Respir J* 2020; 55: 9–11.
5. Rubin GD, Ryerson CJ, Haramati LB, et al. The Role of Chest Imaging in Patient Management During the COVID-19 Pandemic. *Chest* 2020; 158: 106–116.
6. Cleverley J, Piper J, Jones MM. The role of chest radiography in confirming covid-19 pneumonia. *BMJ*; 370. Epub ahead of print 2020. DOI: 10.1136/bmj.m2426.
7. Wen Z, Chi Y, Zhang L, et al. Coronavirus Disease 2019: Initial Detection on Chest CT in a Retrospective Multicenter Study of 103 Chinese Patients. *Radiol Cardiothorac Imaging* 2020; 2: e200092.
8. O' Neill SB, Byrne D, Müller NL, et al. Radiological Society of North America (RSNA) Expert Consensus Statement Related to Chest CT Findings in COVID-19 Versus CO-RADS: Comparison of Reporting System Performance Among Chest Radiologists and End-User Preference. *Can Assoc Radiol J*. Epub ahead of print 2020. DOI: 10.1177/0846537120968919.
9. Salehi S, Abedi A, Balakrishnan S, et al. Coronavirus disease 2019 (COVID-19): A systematic review of imaging findings in 919 patients. *Am J Roentgenol* 2020; 215: 87–93.
10. Sharma R, Agarwal M, Gupta M, et al. Clinical Characteristics and Differential Clinical Diagnosis of Novel Coronavirus Disease 2019 (COVID-19). 2020; 2019: 55–70.

11. Duzgun SA, Durhan G, Demirkazik FB, et al. COVID-19 pneumonia: the great radiological mimicker. *Insights Imaging*; 11. Epub ahead of print 2020. DOI: 10.1186/s13244-020-00933-z.

12. Zhou S, Wang Y, Zhu T, et al. CT features of coronavirus disease 2019 (COVID-19) pneumonia in 62 patients in Wuhan, China. *Am J Roentgenol* 2020; 214: 1287–1294.

13. Liu M, Zeng W, Wen Y, et al. COVID-19 pneumonia: CT findings of 122 patients and differentiation from influenza pneumonia. *Eur Radiol* 2020; 30: 5463–5469.

14. Wang H, Wei R, Rao G, et al. Characteristic CT findings distinguishing 2019 novel coronavirus disease (COVID-19) from influenza pneumonia. *Eur Radiol* 2020; 30: 4910–4917.

15. Shen C, Tan M, Song X, et al. Comparative Analysis of Early-Stage Clinical Features Between COVID-19 and Influenza A H1N1 Virus Pneumonia. *Front Public Heal* 2020; 8: 1–7.

16. Jafari R, Jonaidi-Jafari N, Maghsoudi H, et al. “Pulmonary target sign” as a diagnostic feature in chest computed tomography of COVID-19. *World J Radiol* 2021; 13: 233–242.

17. Mclaren TA, Gruden JF, Green DB. Since January 2020 Elsevier has created a COVID-19 resource centre with free information in English and Mandarin on the novel coronavirus COVID- 19 . The COVID-19 resource centre is hosted on Elsevier Connect , the company ’ s public news and information .

18. Li Y, Xia L. Coronavirus disease 2019 (COVID-19): Role of chest CT in diagnosis and management. *Am J Roentgenol* 2020; 214: 1280–1286.

19. Bai HX, Hsieh B, Xiong Z, et al. Performance of Radiologists in Differentiating COVID-19 from Non-COVID-19 Viral Pneumonia at Chest CT. *Radiology* 2020; 296: E46–E54.

20. Prokop M, Van Everdingen W, Van Rees Vellinga T, et al. CO-RADS: A Categorical CT Assessment Scheme for Patients Suspected of Having COVID-19-Definition and Evaluation. *Radiology* 2020; 296: E97–E104.

21. Fujioka T, Takahashi M, Mori M, et al. Evaluation of the Usefulness of CO-RADS for Chest CT in Patients Suspected of Having COVID-19. *Diagnostics*; 10. Epub ahead of print 2020. DOI: 10.3390/diagnostics10090608.

22. Dilek O, Kaya O, Akkaya H, et al. Diagnostic performance and interobserver agreement of CO-RADS: evaluation of classification in radiology practice. *Diagnostic Interv Radiol* 2021; 27: 615–620.

23. Özel M, Aslan A, Araç S. Use of the COVID-19 Reporting and Data System (CO-RADS) classification and chest computed tomography involvement score (CT-IS) in COVID-19 pneumonia. *Radiol Medica* 2021; 126: 679–687.

24. Abdel-Tawab M, Basha MAA, Mohamed IAI, et al. Comparison of the CO-RADS and the RSNA chest CT classification system concerning sensitivity and reliability for the diagnosis of COVID-19 pneumonia. *Insights Imaging*; 12. Epub ahead of print 2021. DOI: 10.1186/s13244-021-00998-4.

25. Bellini D, Panvini N, Rengo M, et al. Diagnostic accuracy and interobserver variability of CO-RADS in patients with suspected coronavirus disease-2019: a multireader validation study. *Eur Radiol* 2021; 31: 1932–1940.

Table 1.

	Non-COVİD-19	**COVİD-19**	**All Patients**

Averages of ages and standard deviation	49,29±19,43	53,01±15,91	51,99±16,99
Min-Max (Median)	18-84 (53,5)	18-91 (53)	18-91 (53)
Gender			
Female	%41,5 (n=39)	% 40,2 (n=100)	%40,5 (n=139)
Male	%58,5 (n=55)	% 59,8 (n=149)	59,5 (n=204)
Concomitant chronic illness			
Absent	---	%33 (n=113)	
Cardiovascular disease	%3,7 (n=4)	%4,1 (n=14)	
Hypertension	%1,9 (n=2)	%22,5 (n=77)	
Diabetes Mellitus	%5,6 (n=6)	%14,6 (n=50)	
Chronic Lung Disease	%2,8 (n=3)	%1,8 (n=6)	
Chronic Liver Disease	%1,9 (n=2)	%0 (n=0)	
Chronic Kidney Disease	%19,4 (n=21)	%2,3 (n=8)	
Malignancy (extrapulmonary)	%21,3 (n=23)	%3,2 (n=11)	
Conditions Related to Immunodeficiency	%28,7 (n=31)	%3,5 (n=12)	
Others	%14,8 (n=16)	%14,9 (n=51)	

Table 2.

		Group		p
		Non-COVID-19	**COVID-19**	
RSNA Consensus	**Typical**	38 (%40,4)	214 (%85,9)	
	İndetermine	32 (%34)	29 (%11,7)	
	Atypical	24 (%25,5)	6 (%2,4)	
CORADS	**CORADS 2 /Low**	27 (%28,7)	7 (%2,8)	
	CORADS 3/İndetemine	30 (%31,9)	17 (%6,8)	**0,001****
	CORADS 4 /High	12 (%12,8)	31 (%12,4)	
	CORADS 5 /Very high	25 (%26,6)	194 (%77,9)	
Percentage of Involvement	**%0-%25**	32 (%34)	107 (%43)	
	%25-%50	29 (%30,9)	97 (%39)	
	%50-%75	17 (%18,1)	34 (%13,7)	
	%75<	16 (%17)	11 (%4,4)	
Number of lesions				**0,022***
	Single	1 (%1,1)	17 (%6,8)	
	Multiple	93 (%98,9)	232 (%93,2)	
Distribution Preference				**0,001****
	Peripheral	11 (%11,7)	101 (%40,7)	
	Central	2 (%2,1)	2 (%0,8)	
	Peripheral+ Central	81 (%86,2)	145 (%58,5)	
Dominant Pattern				
	GGO	53 (%56,4)	196 (%78,7)	**0,001****
	Consolidation	13 (%13,8)	46 (%18,5)	
	Linear, Reticular Opacity	2 (%2,1)	3 (%1,2)	
	Nodule	26 (%27,7)	4 (%1,6)	

		Group		p
		Non-COVID-19	**COVID-19**	
Distribution pattern of GGO	**Absence (-)**	10 (%10,6)	3 (%1,2)	**0,001****
	Peripheral-bilateral	19 (%20,2)	140 (%56,2)	
	Round-multifocal	20 (%21,3)	68 (%27,3)	
	Halo Sign	1 (%1,1)	0 (%0)	
	Diffuse	26 (%27,7)	4 (%1,6)	
	Perihilar-not round	5 (%5,3)	3 (%1,2)	
	Single sided-Not Round	13 (%13,8)	31 (%12,4)	
Nodule		56 (%60,6)	12 (%4,8)	**0,001****
Tree In Bud Pattern		49 (%52,1)	8 (%3,2)	**0,001****
Interstitial Changes	**Absent**	24 (%25,5)	60 (%24,1)	**0,001****
	Septal Thickening	33 (%35,1)	17 (%6,8)	
	Fine Reticular Opacity	7 (%7,4)	72 (%28,9)	
	Septal Thickening + Fine Reticular Opacity	30 (%31,9)	100 (%40,2)	
'Crazy Paving' Pattern		13 (%13,8)	76 (%30,5)	**0,001****
Reversed Halo (Atoll)		6 (%6,4)	109 (%43,8)	**0,001****
Microvascular Enlargement		60 (%63,8)	207 (%83,1)	**0,001****
Linear Opacities		71 (%75,5)	157 (%63,1)	**0,029***
Traction Bronchiectasis		45 (%47,9)	155 (%62,2)	**0,016***
		Non-COVID-19	**COVID-19**	**p**

Peribronchial Wall Thickening		55 (%58,5)	82 (%32,9)	**0,001****
Air Trapping		31 (%33)	29 (%11,6)	**0,001****
Pleural Retraction		54 (%57,4)	99 (%39,8)	**0,001****
Pleural Effusion		31 (%33)	8 (%3,2)	**0,001****
Pericardial Effusion		28 (%29,8)	9 (%3,6)	**0,001****
Cavitation		3 (%3,2)	0 (%0)	**0,001****
Mediastinal-Hilar Lymph Node	**Nonspecific**	65 (%69,1)	229 (%92)	**0,001****
	Pathological	28 (%29,8)	20 (%8)	
	Another Reason	1 (%1)	0 (%0)	
Dominant Lesion Size				
	0-3 cm	43 (%45,7)	85 (%34,1)	
	3-5 cm	10 (%10,6)	46 (%18,5)	0,122
	5-7 cm	8 (%8,5)	30 (%12)	
	>7 cm	33 (%35,1)	88 (%35,3)	
Consolidation		52 (%55,3)	137 (%55)	0,960
Vacuolar Sign		11 (%11,7)	22 (%8,8)	0,270
Halo Sign		19 (%20,2)	60 (%24,2)	0,436
Subpleural Curvilinear Opacity		23 (%24,5)	75 (%30,1)	0,301
Air Bronchogram		23 (%24,5)	49 (%19,8)	0,340
Pleural Thickening		19 (%20,2)	54 (%21,7)	0,766

Chi-Square Testi ****p<0,01**

Table 3. Multiple Regression Analysis Findings in Relation of Independent Variables to COVID-19

Model	Variables	B	S. Error	β	p
1	Constant	1,078	115344,8	2,939	0,999
	Percentage of Involvement-%0-%25	-0,512	1,538	0,599	0,739
	Percentage of Involvement-%25-%50	0,07	1,207	1,073	0,954
	Percentage of Involvement-%50-%75	-0,962	1,12	0,382	0,39
	Percentage of Involvement-%75<	-0,714	1,028	0,49	0,487
	Number of lesions - Single	-18,856	8494,375	0	0,998
	Transverse Distribution Peripheral	13,089	40192,85	483558,2	0,999
	Transverse Distribution Central	7,533	40192,85	1869,159	0,999
	Transverse Distribution Peripheral+Central	13,342	40192,85	622821,2	0,999
	Dominant Pattern - GGO	-22,783	22512,07	0	0,999
	Dominant Pattern - Consolidation	-26,04	22512,07	0	0,999
	Dominant Pattern - Linear,Reticular Opacity	-23,08	22512,07	0	0,999
	Dominant Pattern - Nodule	-23,966	22512,07	0	0,999
	GGO Peripheral-bilateral	1,083	1,363	2,955	0,427
	GGO Round-multifocal	-1,24	1,023	0,289	0,225
	GGO Halo Sign	0,377	1,066	1,457	0,724
	GGO Diffuse	22,949	9516,478	9,26E+09	0,998
	GGO Perihilar-not round	1,507	1,34	4,514	0,261
	GGO SingleSided-Not Round	1,533	6,119	4,633	0,802
	Nodule	2,308	1,307	10,052	0,078
	Tree In Bud Pattern	1,316	1,354	3,727	0,331
	Interstitial Changes absent	0,231	0,958	1,26	0,809
	İnterstisyel Changes Septal Thickening	1,021	0,826	2,777	0,216
	Interstitial Changes Fine Reticular Opacity	-0,463	0,87	0,63	0,595
	Crazy Paving Pattern	-0,454	0,833	0,635	0,586
	Reversed Halo	**-2,334**	**0,952**	**0,097**	**0,014***
	Microvascular Enlargement	-0,203	0,614	0,816	0,741
	Linear Opacities	-0,73	0,733	0,482	0,319
	Traction Bronchiectasis	-0,23	0,603	0,794	0,703
	Peribronchial Wall Thickening	0,561	0,512	1,753	0,273
	Air Trapping	1,222	0,621	3,394	0,055

Pleural Retraction	1,063	0,614	2,895	0,083
Pleural Effusion	**2,364**	**0,743**	**10,631**	**0,001****
Pericardial Effusion	0,774	0,722	2,168	0,284
Cavitation	44,133	19385,62	1,47E+19	0,998
Mediastinal-Hilar Lymph Node - Nonspecific	-3,993	41304,74	0,018	0,999
Mediastinal-Hilar Lymph Node - Pathological	-3,184	41304,74	0,041	0,999

R^2= 0,793

$X^2_{(1,51)}$=130,451, p=0,001**

*p<0,05 **p<0,01

Figure Legends

Figure 1. A female patient in her 70s, diagnosed with HCoV-OC43 pneumonia, chronic lymphocytic leukemia (CLL). According to the RSNA guidelines 'typically', the CORADS score was evaluated as 5. GGO (crazy paving) (black arrow) accompanied by interlobular and intralobular septal thickening on the axial CT section and patchy consolidation areas, faint GGO areas (black arrowhead); pleural effusion (asterisks).

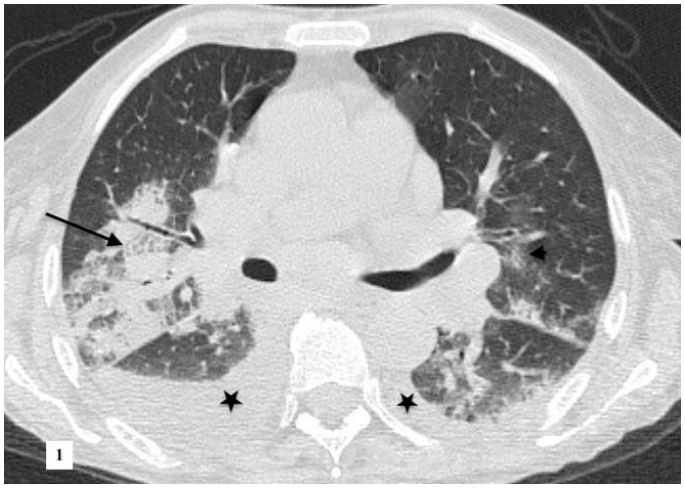

Figure 2. A male patient in his 50s, with COVID-19 pneumonia, known history of hypertension. 'Typical' according to RSNA guidelines, CORADS score was evaluated as 5. Bilateral widespread subpleural curvilinear opacities are demonstrated (black arrows).

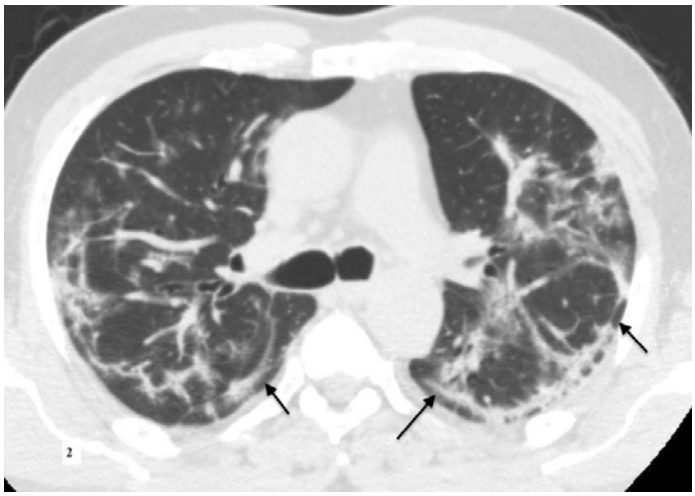

Figure 3. A male patient in his 30s, with influenza B pneumonia, diagnosed with known end-stage renal disease. The score was evaluated as 2 according to the CORADS classification and in the atypical group according to the RSNA guidelines. Soft tissue density centrilobular nodules (black arrow) forming tree in bud pattern and peribronchovascular consolidation.

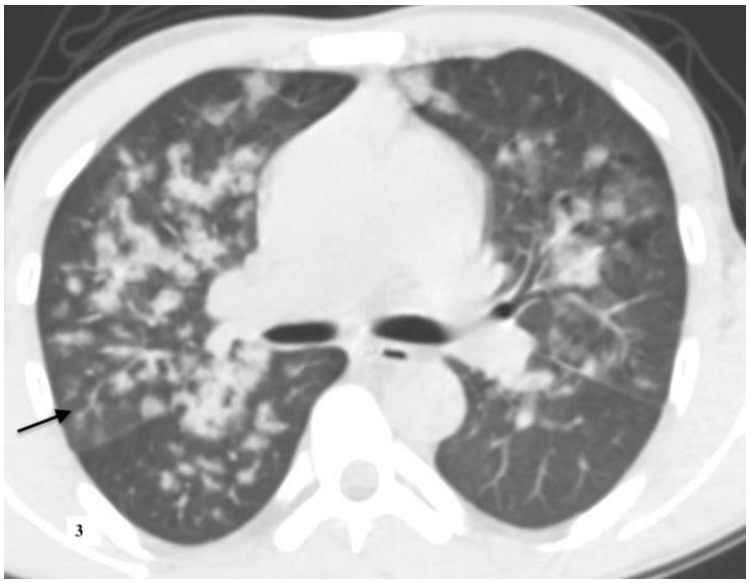

Figure 4. A female patient in her 60s, with influenza A (H1N1) pneumonia, known diabetes, chronic kidney disease. According to the RSNA guidelines in the typical group, the score 5 was evaluated in the CORADS classification. Bilateral rounded consolidation areas (black arrows) and parenchymal band (black arrowhead) are observed.

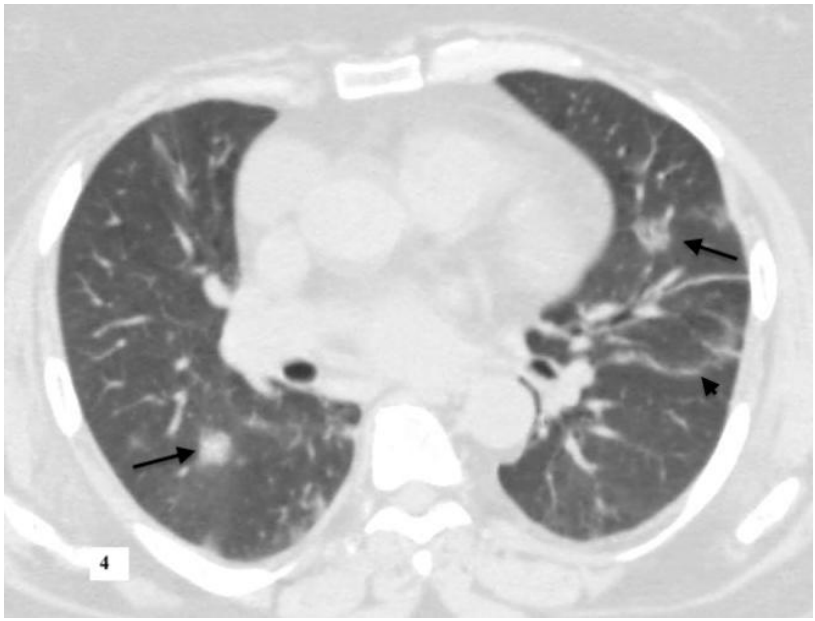

Figure 5. An female patient in in the late 2nd decade, with parainfluenza (HPIV 3) pneumonia, with bone marrow transplantation due to acute lymphoblastic leukemia. According to the RSNA guidelines in 'indetermine', CORADS score was evaluated as 3. Diffuse centrilobular ground glass density nodules (black arrow) and focal peripheral consolidation areas (black arrowhead), increased peribronchial wall thickness (white arrowhead) are observed.

Figure 6. A male patient in his 30s, with COVID-19 pneumonia, known diagnosis of asthma. 'Typical' according to RSNA guidelines, CORADS score was evaluated as 5. Bilateral lung parenchyma rounded, multifocal GGO lesions (black arrows); reversed halo sign (white arrow) central part is relative normal, with GGO in the periphery are observed.

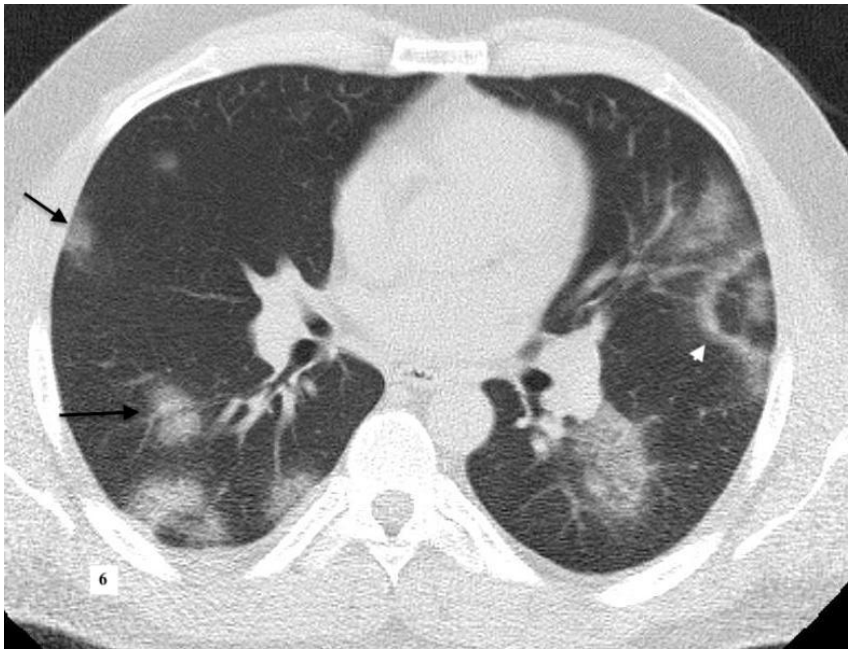

Figure 7. A male patient his 20s, diagnosed with known primary immunodeficiency with adenovirus pneumonia. According to the RSNA guidelines 'indetermine', CORADS score was evaluated as 4. İrregular peripheral consolidation (black arrows) and increased peribronchial thickness (white arrowhead) are observed.